# A Statistical Study of CMEs Associated with Metric Type II bursts

A. Lara,[1] N. Gopalswamy,[2] S. Nunes,[2,3] G. Muñoz,[1] and S. Yashiro[2,3]

---

A. Lara, Instituto de Geofísica, UNAM, México D.F. 04510 México. (alara@igeofcu.unam.mx)

N. Gopalswamy, Code 695.0, Bldg 21, Room 260, NASA/GSFC, Greenbelt, MD 20771-0001. (gopals@fugee.gsfc.nasa.gov)

[1]Instituto de Geofísica, UNAM, México.

[2]NASA/GSFC, Greenbelt MD, USA.

[3]The Catholic University of America, Washington DC 20064, USA.

**Abstract.** We present a statistical study of the characteristics of CMEs which show temporal association with type II burst in the metric domain but not in the decameter/hectometric (DH) domain. This study is based on a set of 80 metric type II bursts associated with surface events in the solar western hemisphere. It was found that in general, the distribution of the widths and speeds of the CMEs associated with metric (but no DH) type II bursts are shifted towards higher values compared to those of all CMEs observed by LASCO in the 1996-2001 period. We also found that these distributions have lower values than the same distributions of the CMEs associated with DH type II bursts. In terms of energy, this means that the CMEs associated only with metric type II bursts are more energetic (wider and faster) than regular CMEs but less energetic than the CMEs associated with DH type II bursts.

## 1. Introduction

Type II radio bursts are electromagnetic emissions which show a relatively slow drift in the dynamic spectra (frequency - time plots). These emissions are associated with disturbances moving in the solar atmosphere. It is generally accepted that the emitting frequency is approximately equal to the local plasma frequency ($f$) (or its harmonic) which is related to the the ambient density ($n$) in the form $f[\text{kHz}] \sim 9\sqrt{n}[\text{cm}^{-3}]$. The movement of the disturbance through different density levels can be "traced" by the radio emission. Depending on the wavelength regime of observation, Type II bursts are grouped into metric type II, decameter/hectometric and kilometric bands. The densities associated with these bands corresponds approximately to helio centric altitudes lower than $\sim 2$, between $\sim 2$ and $\sim 10$ and higher than $\sim 10$ solar radii, respectively.

Extensive literature is available on the origin and relationship between type II bursts in the metric, DH and kilometric regimes. While it is widely accepted that the DH and kilometric type IIs are caused by coronal mass ejection (CME) driven shocks, it is a controversial for metric type II bursts. There are at least three possibilities for the origin of metric type II bursts.

1. The same origin as the DH type II, i. e., the CME-driven shock produce the metric type II when it is at very low altitudes and the DH type II at higher altitudes. In this case we should expect a high association between the two phenomena, at least for fast CMEs.

2. A shock formed behind the CME can also produce a metric type II. This shock can be formed, for instance, when the upper part of a fast jet formed in the reconnection region reaches the lower part of the CME. In this case we should expect a high association

between metric type IIs and low atmospheric manifestations of the jet, such as H$\alpha$ or X-ray emissions.

3. A shock driven by a blast wave produced by a flare can also be the exiting agent that produces the metric type II bursts. In this case an association between flare importance and metric type II bursts is expected.

The primary objection to the CME origin of metric type II bursts has been the poor correlation between metric and DH type II bursts [*Gopalswamy et al.*, 1998; *Cliver*, 1999; *Cliver, Webb and Howard,* 1999]. Recently, Gopalswamy et al. [2001a] suggested that it is possible to resolve the controversy if one takes into account of the radial profile of the Alfvén speed. They found that between 3 and 4 $R_\odot$, the Alfvén speed peaks and hence acts as a filter that removes all weak shocks beyond this region. According to this idea, it is easy to form shocks in the inner corona (below 1.5 $R_\odot$) which produce metric type II bursts. When these shocks approach the Alfvén speed peak region, they decay as MHD waves. Depending on the speed of the CMEs, a second shock may be set up beyond the Alfvén speed peak to produce DH type II bursts. Gopalswamy and Kaiser [2002] demonstrated this using the metric and DH type II bursts of the 1997 May 12 Event. Another implication of this Alfvén speed peak is that accelerating CMEs that attain superAlfvenic speeds only in the outer corona may not produce metric type type II burst at all. To confirm this result for a large number of events, we decided to study all the metric type II bursts that were not followed by DH type II bursts. We shall explore the characteristics of CMEs associated with these metric type II bursts and compare them with those associated with DH type II bursts.

## 2. Data and Analysis

The time period covered by this study ranges from June 1996 to October 2001. We chose the metric type II burst based on the following criteria: 1. they originated from the western hemisphere, and 2. they are not associated with DH type II bursts. The solar sources were identified from the solar geophysical data based on the locations of associated H-alpha flares. The reason for choosing the western hemispheric events is to study the relation between metric type II bursts and solar energetic particle events, which will be reported elsewhere. The reason for choosing metric type II bursts without DH type II bursts is to understand the primary difference between the two populations. With this criteria, we identified 145 metric type II bursts.

The CME data used in this study were obtained by the Solar and Heliospheric Observatory (SOHO) mission's Large Angle and Spectrometric Coronagraph (LASCO) All CMEs observed from the launch of SOHO until the end of 2001 are listed in an on-line catalog (http://cdaw.gsfc.nasa.gov). Unfortunately, 18 metric type II bursts occured during LASCO data gaps, this fact reduces our data set to 127 events.

### 2.1. Onset times of CMEs and Type II bursts.

Allowing a time window of three hours immediately following the metric onset time, we found 93 CMEs (73%) that could be associated with these metric type II bursts. We note that 21 ($\sim$ 62%) and 28 ($\sim$ 82%) out of 34 events which have not apparent CME association have a Helio-longitude lower than 45° and 60°, respectively. This lack of association may be due to the poor visibility of CMEs originating from the disk center. Additionally, we dropped 13 events because the difference between the position angle (PA) of the associated solar source and the PA of the CMEs were greater than 120°.

Extrapolating the second order fit of the CME height-time data, we are able to compute the time when each CME was at a height of one solar radius ($t_{1R_\odot}$) from the Sun center. In order to determine if the CMEs are related to the observed metric type II burst we compare the $t_{1R_\odot}$ with the metric type II onset time ($t_{m-TII}$). Figure 1 shows the histogram of the $t_{1R_\odot}$ - $t_{m-TII}$ differences. The peak (and mean) of the distribution is at -0.2 hrs. This results reflects a very high association between the two phenomena. More over, figure 2 shows the dependence of the time difference ($t_{1R_\odot}$ - $t_{m-TII}$) as a function of the Helio-longitude. As expected, the time difference is lower for the limb events.

### 2.2. Comparison of Metric and DH type II Properties

For this study, we compiled the width, speed and acceleration of three populations of CMEs: 1. The CMEs associated with the metric type II bursts selected for this study. 2. The general population of CMEs (5117 in number) observed by SOHO/LASCO during January 1996 to the end of 2001 as listed in the on-line catalog (http://cdaw.gsfc.nasa.gov). 3. The CMEs associated with DH type II bursts as published in Gopalswamy et al. [2001b].

Figures 3, 4 and 5 show the distributions of widths, speeds and acceleration, respectively, for the three populations of CMEs: the general population (g-CMEs) in black bars, the metric type II associated (m-CMEs) in gray bars and the DH associated (DH-CMEs) in white bars.

The actual width of halo CMEs ($> 200°$) is difficult to measure due to geometrical effects (see Gopalswamy et al. 2001). Then we exclude halo CMEs for the width analysis. Figure 3 shows the distribution of the widths of 4845 ($\sim 95\%$) non halo CMEs (black) of the g-CMEs. This distribution is asymmetric and shows a peak $\sim 50°$. The mean width is $\sim 56°$. The distribution of the 75 (out of 80, i.e., 93%) non halo m-CMEs (gray) has a peak at $\sim 70°$ and tends to be more symmetrical than the g-CME distribution. In this case, the mean width is $\sim 90°$. The distribution of the 45 non-halo DH-CMEs (white) peaks at $\sim 100°$, and has a mean value of $\sim 102°$. Thus the average width progressively increases from g-CMEs to m-CMEs to DH-CMEs.

The speed distribution (Figure 4) shows a peak around 350 km/s for the g-CMEs, and a higher speed peak, $\sim$ 450 km/s, for the m-CMEs. The DH-CME speed distribution is somewhat flat showing two peaks at $\sim$ 650 and $\sim$ 1050 km/s. The mean values are: 455, 545 and 964 km/s for the general, metric and DH CMEs respectively. The progression is very similar to the width distributions.

The acceleration distributions (Figure 5) are more symmetrical. The acceleration distribution of g-CMEs has a peak around 5 $m/s^2$ and its mean is $\sim -0.5$ $m/s^2$. On the other hand, both the m-CMEs and DH-CMEs acceleration distributions peak at -5 $m/s^2$. The mean acceleration are $\sim -6.1$ and $\sim -7.8$ $m/s^2$ for the m-CMEs and DH-CMEs, respectively. Thus, while the g-CMEs show no significant acceleration, the m-CMEs and DH-CMEs show significant deceleration. The deceleration is largest for the DH-CMEs.

## 3. Discussion and Conclusions

The origin of metric type II burst has been an open question that have been discussed during decades [see e.g. the reviews by *Gopalswamy et al.*, 1998; *Cliver, Webb and Howard*, 1999]. In particular, the association of metric type II bursts and fast ejection was established since the early studies of the subject [*Dodson, Hedeman and Chamberlain*, 1953]. Although, the CME driven shock origin of the type II bursts is not widely accepted [*Uchida*, 1968, 1974; *Maxwell and Dryer*, 1982; *Cane*, 1983]. One of the reasons for these discrepancies is the high number of observed CMEs and the low number of observed Type II burts. To solve this problem, it was necessary to invoke special conditions and/or a special kind of CMEs that produces type II bursts [see *Cliver, Webb and Howard*, 1999, and references therein]. In this sense it was showed by Gosling et al. [1976] that type II burst were highly associated with fast CMEs ($>$ 400 km/s). Recently, Goplaswamy et al. [2001] showed that all DH type II bursts are associated with fast and wide CMEs. In an inverse study, they also found a number of fast CMEs ($>$ 900 km/s) without associated DH type II bursts. The distinguishing characteristic between CMEs with and without type II bursts was found to be the width of the CMEs. i.e., narrow CMEs did not produce DH type II even though they were fast. In this study we found that there are special characteristics that distinguish CMEs associated with metric type II bursts compared with CMEs associated with DH type II bursts and the characteristics of the general population of CMEs.

We confirm that the CMEs associated with metric Type II bursts are faster ($\sim$ 450 km/s) than the common CMEs ($\sim$ 350 km/s), but we found that are slower than the CMEs associated with DH type II bursts. In terms of width we found a similar behavior, i. e., the width of the general CMEs ($\sim 50^{\circ}$) is lower than the width of the metric type II associated CMEs ($\sim 70^{\circ}$) and in turn this is lower than the average width of the DH type II bursts associated CMEs ($\sim 100^{\circ}$).

Taking into account that the combination of speed and width of CMEs reflects their energy, it is reasonable to think that the CME energy as the major factor which "control" the type II burst production. A very small energy CME will not produce a type II at all. The probability of a medium energy CME to produce a type II burst in the low corona is high, but is possible that only the most energetic CMEs have enough power to produce also DH type II bursts. Note that we need more information than just the energy to understand the relation between metric and DH type II bursts. To produce type II bursts, the CME has to drive a shock. Low energy CMEs can drive a shock close to the Sun, but may or may not drive a shock at 3-4 $R_\odot$ because of the Alfvén speed distribution in the radial direction away from the Sun [*Gopalswamy et al.*, 2001a]. Thus, a combination of the CME energy and the Alfvén speed profile decide the production of type II bursts in various domains.

The measured acceleration of both metric and DH associated CMEs tends to be negative compared with the acceleration of the total number of CMEs (the average values are $\sim -6.0$, $\sim -7.8$ and $\sim -0.5$ m/s$^2$, respectively). This supports the idea that the CMEs are loosing kinetic energy due to the interaction with the ambient corona [*Gopalswamy et al.*, 2000; 2001c]. The acceleration distribution confirms the importance of the CME speed and width because both of these quantities determine the coronal drag that decelerates CMEs. This explain way not all CMEs will drive a shock in the low corona and near Sun interplanetary space.

**Acknowledgments.**

This research was partially supported by CONACyT grant 33321-E. SOHO is a project of international cooperation between ESA and NASA. SN and SY are supported by AFOSR and NASA grants to the Catholic University of America, Washington DC.

## References

Cane, H. V., in M. Neugebauer (ed.), *Solar Wind Five*, NASA, 703, 1983.

Cliver, E. W., *J. Geophys. Res.*, **104**, 4743, 1999.

Cliver, E. W.; Webb, D. F. and Huward, R. A, On the Origin of Solar Metric Type II Bursts, *Sol. Phys.*, **187**, 89, 1999.

Dodson, H. W.; Hedeman, E. R. and Chamberlain, J., *Astrophys. J.* **117**, 16, 1953.

Gopalswamy, N. et al., *J. Geophys. Res.*, **103**, 307, 1998.

Gopalswamy, N. et al., *J. GRL*, **27**, 1427, 2000.

Gopalswamy, N., Lara, A., Kaiser, M. L., & Bougeret, J.-L., "Near-Sun and near-Earth manifestations of solar eruptions", *J. Geophys. Res.*, **106**, 25261, 2001a.

Gopalswamy, N.; Yashiro, S.; Kaiser, M. L.; Howard, R. A. and Bougeret, J., *J. Geophys. Res.*, **106**, 29219, 2001b.

Gopalswamy,N.; Yashiro,S.; Kaiser,M.L.; Howard,R.A. and Bougeret,J.-L, *The Astrophys. J.*, **548**, 91, 2001c.

Gopalswamy, N. & Kaiser, M. L., "Solar eruptions and long wavelength radio bursts: The 1997 May 12 event", *Adv. Space Res.*, **29**, 307, 2002.

Gosling, J. T., Hildner, E., MacQueen, R. M., Munro R. H., Poland, A. I. and Ross, C. L., *Sol. Phys.*, **48**, 379, 1976.

Maxwell, A. and Dryer, M., *Space Sci. Rev.*, **32**, 11, 1982.

Uchida, Y., *Sol. Phys.*, **4**, 30, 1968.

Uchida, Y., *Sol. Phys.*, **39**, 431, 1974

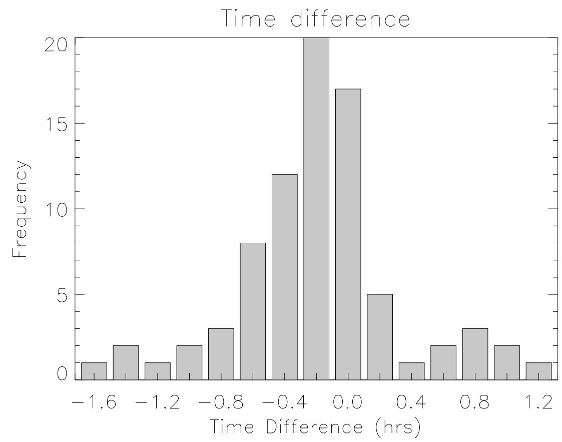


**Figure 1.** Histogram (with a bin size is 0.2 hrs.) of the differences between the time when the CME was at 1 $R_\odot$ (computed assuming the speed and acceleration measured in the LASCO field of view) and the metric type II onset time.

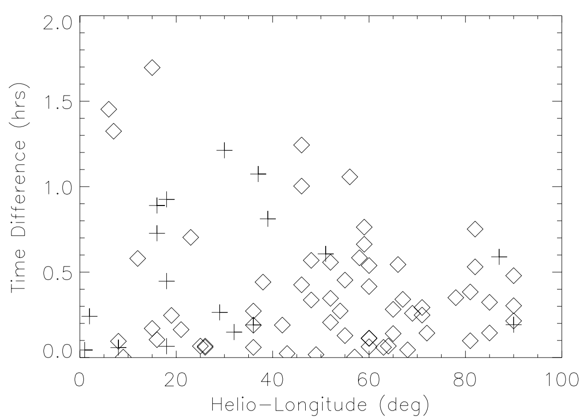


**Figure 2.** Time difference (see Fig. 1) as a function of the Helio-longitude positive (negative) differences are marked with plus (diamonds) symbols.

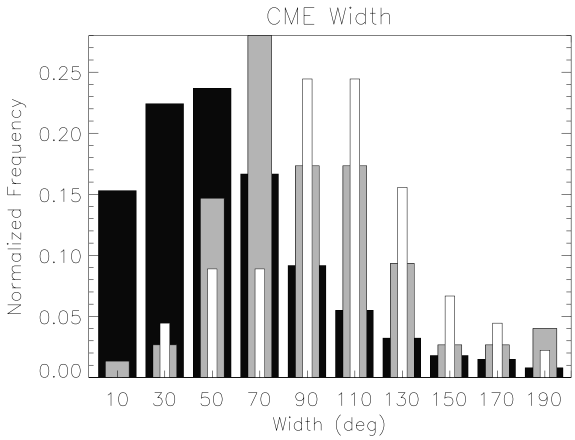


**Figure 3.** Histogram (with a bin size is 20°) of the widths of; i) 4880 non halo CMEs observed by LASCO (black bars); ii) 75 CMEs associated with metric but not DH type II bursts (gray bars) and iii) 45 CMEs associated with DH type II bursts (white bars).

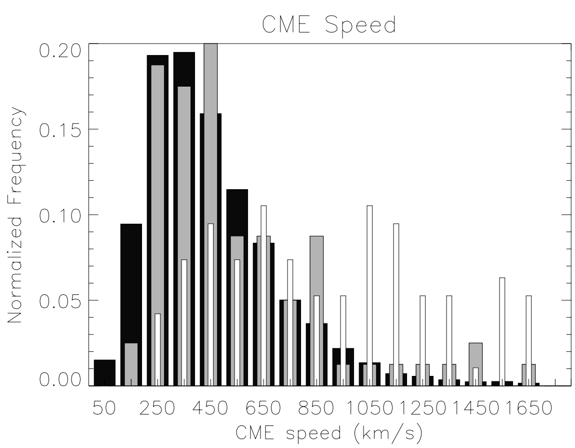


**Figure 4.** Histogram (with a bin size is 100 km/s) of the plane of the sky measured speed of; i) 5156 CMEs observed by LASCO (black bars); ii) 78 CMEs associated with metric but not DH type II bursts (gray bars) and iii) 101 CMEs associated with DH type II bursts (white bars).

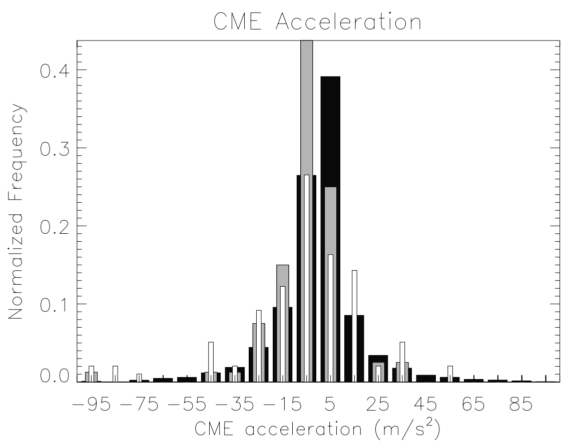


**Figure 5.** Same as figure 4 for the measured accelerations.